Inorganic Chemistry

Article

pubs.acs.org/IC

Probing Highly Selective H/D Exchange Processes with a Ruthenium Complex through Neutron Diffraction and Multinuclear NMR Studies.

Mary Grellier,*[,†,‡] Sax A. Mason,[§] Alberto Albinati,*[,∥] Silvia C. Capelli,[§] Silvia Rizzato,[∥] Christian Bijani,[†,‡] Yannick Coppel,[†,‡] and Sylviane Sabo-Etienne*[,†,‡]

[†]CNRS, LCC (Laboratoire de Chimie de Coordination), 205 route de Narbonne, BP 44099, F-31077 Toulouse Cedex 4, France

[‡]Université de Toulouse, UPS, INPT, F-31077 Toulouse Cedex 4, France

[§]Institut Laue-Langevin, 6 rue Jules Horowitz, BP 156, 38042 Grenoble Cedex 9, France

[∥]Dipartimento di Chimica, Università di Milano, Via C. Golgi, 19, 20133 Milan, Italy

Supporting Information

ABSTRACT: Deuterium labeling is a powerful way to gain mechanistic information in biology and chemistry. However, selectivity is hard to control experimentally, and labeled sites can be difficult to assign both in solution and in the solid state. Here we show that very selective high-deuterium contents can be achieved for the polyhydride ruthenium phosphine complex $[RuH_2(H_2)_2(PCyp_3)_2]$ (**1**) ($PCyp_3 = P(C_5H_9)_3$). The selectivity of the H/D exchange process is demonstrated by multinuclear NMR and neutron diffraction analyses. It has also been investigated through density functional theory (DFT) calculations. The reactions are performed under mild conditions at room temperature, and the extent of deuterium incorporation, involving selective C−H bond activation within the cyclopentyl rings of the phosphine ligands, can easily be tuned (solvent effects, D_2 pressure). It is shown that D_2 gas can inhibit the C−H/C−D exchange process.

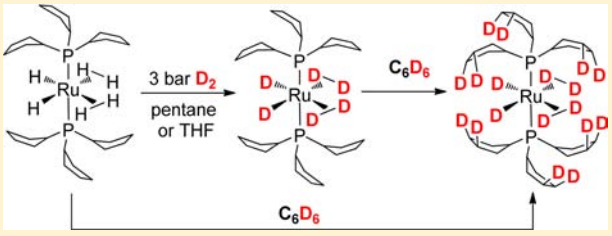

INTRODUCTION

Deuterium incorporation into a wide range of substrates is a process of high interest both for synthetic applications and mechanistic investigations.[1] Deuterium labeled compounds are used routinely as NMR solvents and are seeing increasing demand as internal standards for mass spectrometry and protein structure determination. Kinetic isotope effects are widely used to investigate a large panel of reactions with applications in biology, and in organic and inorganic chemistry.[2] Organometallic chemistry has benefited tremendously from studying H/D exchange reactions to gain mechanistic information.[3] As the field of catalytic C−H bond functionalization undergoes dramatic growth, such labeling studies become more and more useful.[4] One of the major challenges in this area is to control the H/D exchange. Very often there is isotopic scrambling, making definitive conclusions quite difficult. Such scrambling may have several causes: (*i*) the source of deuterium might play a role as well as the nature of the catalyst precursor, (*ii*) hydrogen bonds can interfere in the process and are hard to control, (*iii*) knowledge of kinetic effects is limited, (*iv*) concurrent reactions in metal-catalyzed H/D exchange may play a role. In solution, NMR spectroscopy is definitely the best tool to analyze H/D exchange processes. ^{1}H NMR experiments are used routinely and ^{2}H NMR measurements are readily accessible despite a loss of sensitivity relative to ^{1}H of 1.45×10^{-6} and a less favorable nuclear spin of 1. In the solid state, single-crystal neutron diffraction is a unique tool as it provides not only accurate location of the H atoms but allows unambiguously distinguishing hydrogen from deuterium because of their very different scattering lengths (− 3.7409 vs +6.674 fm). This property has rarely been used as neutron diffraction required, because of flux limitation of the sources, large single crystals. However, recent advances in neutron instrumentation now allow the use of much smaller crystal sizes ($\leq$1 mm^3), and this technique may become a powerful complement to NMR techniques.[5]

Platinum group transition metal complexes are the best catalyst precursors for homogeneous H/D exchange reactions, with iridium being the most important metal used in this area.[6] In many systems, H/D exchange involves hydride species at least as intermediates (in the case of ruthenium, see for example refs 7), but other ligands around the metal center can participate in, and sometimes complicate, the H/D pathways. Transition metal catalysts often incorporate phosphine ligands which are usually considered to be spectator ligands. However, accumulating evidence shows that one can benefit from C−H activation within "non-innocent" ligands such as phosphines to build innovative systems for hydrogen storage applications.[8] A few years ago,[9] we prepared the bis(dihydrogen) complex $[RuH_2(H_2)_2(PCyp_3)_2]$ (**1**) stabilized by two tricyclopentylphosphines ($PCyp_3 = P(C_5H_9)_3$) which was found to display

Received: October 23, 2012
Published: December 20, 2012

   dx.doi.org/10.1021/ic302307m | *Inorg. Chem.* 2013, 52, 7329−7337

properties different from its analogue $[RuH_2(H_2)_2(PCy_3)_2]$ (**2**) which incorporates two tricyclohexylphosphines (PCy_3 = $P(C_6H_{11})_3$).[10] Before describing our investigation on the exchange labeling, it is worth emphasizing some key differences we have observed between **1** and **2**. Simply reducing the size of the cycloalkyl rings led to a very different dehydrogenation process in the reaction with ethylene. In the case of **1** the final product was the ruthenium (0) compound $[Ru(C_2H_4)\{(\eta^2\text{-}C_5H_7)PCyp_2\}_2]$ (**3**) with two partially dehydrogenated phosphines,[11] whereas exposure of ethylene to **2** led to the formation of the ruthenium(II) hydrido complex $[RuH\{(\eta^3\text{-}C_6H_8)PCy_2\}(C_2H_4)(PCy_3)]$ (**4**) in which one phosphine was partially dehydrogenated and coordinated to the metal center in an allylic fashion,[12] as illustrated in Scheme 1. These findings

Scheme 1. Reactivity of 1 and 2 with Ethylene: Two Different Dehydrogenation Pathways

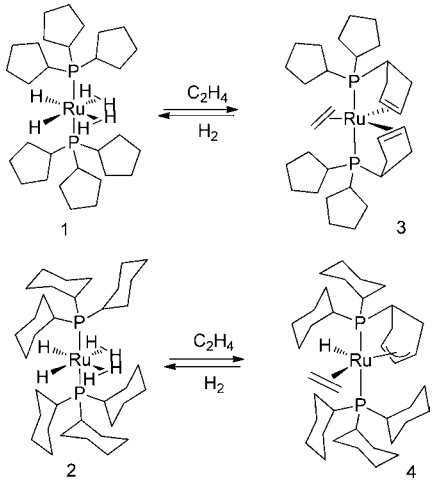

highlight the role of the ancillary ligands, here the phosphines, in hydrogen transfer processes.[13] With respect to catalysis, **1** proved to be much more active than **2** for the hydrogenation of nitriles,[14] or the C−C coupling of functionalized arenes through C−H activation.[9,15]

We present here the results of our study on H/D exchange processes in ruthenium polyhydride chemistry. This is the first report of highly selective deuterium incorporation demonstrated both in the solid state by neutron diffraction and in solution by multinuclear NMR data. Density functional theory (DFT) studies helped to rationalize the mechanism of the different H/D exchange pathways. The phenomenon is directly relevant to catalysis, and in particular to C−H activation and dehydrogenation processes.

RESULTS AND DISCUSSION

The syntheses of **1** and **2** were performed similarly, by addition of 2 equiv of the corresponding phosphine to a pentane solution of Ru(COD)(COT) under 3 bar dihydrogen.[9,12] **1** and **2** could both be isolated as white solids, and displayed similar spectroscopic and structural features. **1** was characterized by neutron diffraction,[9] while **2** was structurally characterized by X-ray diffraction.[16] In solution (C_6D_6 or C_7D_8), the hydride and dihydrogen ligands of **1** and **2** exchanged rapidly at all temperatures giving rise to a ^{1}H NMR signal close to δ −8. However, one striking difference was immediately observed upon dissolution. Not only was **1** more soluble in C_6D_6 than **2**, but rapid H/D exchange could be detected (see Supporting Information, Figures S15−S16), whereas 24 h was necessary in the case of **2** to detect some deuterium incorporation at the hydride sites. The H/D exchange process in the case of **1** turned out to be very selective depending on the experimental conditions (Scheme 2). As discussed below, several factors

Scheme 2. Selective H/D Exchange Processes from Complex 1

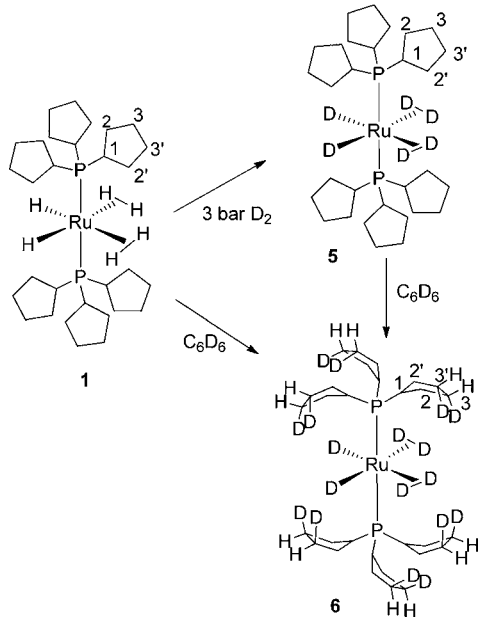

control the H/D exchange process, but two well-defined stages of deuterium incorporation can be achieved: the hydride and dihydrogen sites are deuterated, and deuterium incorporation is also observed in the cyclopentyl rings of the phosphines, with very high site-selectivity.

Selective Deuteration at the Hydride and Dihydrogen Sites. Synthesis and Characterization of $[RuD_2(D_2)_2(P(C_5H_9)_3)_2]$ (5). Exposure of a pentane solution of **1** to 3 bar D_2 over a day (through three cycles of vacuum/3 bar D_2) afforded $RuD_2(D_2)_2(P(C_5H_9)_3)_2$ (**5**) which was isolated as a white solid in 84% yield. The selectivity of the deuteration process was demonstrated in solution by multinuclear NMR studies, and in the solid state by single crystal neutron diffraction. It should be noted that a similar deuteration incorporation was observed in the case of the tricyclohexylphosphine system leading to $RuD_2(D_2)_2(P(C_6H_{11})_3)_2$.[17] Crystals suitable for neutron diffraction were obtained from a pentane solution at −37 °C. NMR spectra were recorded immediately after dissolving **5** in C_6D_6. The ^{1}H NMR spectrum shows a multiplet at δ −8.04 assigned to some residual ^{1}H at the hydride and dihydrogen sites. Integration with the $PCyp_3$ signals at low field (δ 1.6−2.0) gave a deuterium incorporation of 97% for the high field signal (see Supporting Information, Figure S1a,b). ^{2}H NMR spectra confirm that deuteration occurred almost quantitatively for the metal bonded hydrogen atoms with one intense signal observed at δ −8.0 and traces at δ 1.7 (Supporting Information, Figure S2). This is also confirmed by several ^{13}C selective decoupling experiments and most notably a $^{13}C\{^1H,^{31}P\}$NMR spectrum showing no deuterium coupling for the three carbon signals at δ 40.07 (s, PCH, $PCyp_3$), δ 30.34 (s, PCH-$\underline{C}H_2$, $PCyp_3$), and δ 26.66 (s, PCH−CH_2-$\underline{C}H_2$, $PCyp_3$) (Supporting Information, Figure S3).

dx.doi.org/10.1021/ic302307m | Inorg. Chem. 2013, 52, 7329−7337

An ORTEP view of the low T (20 K) neutron diffraction structure of **5** is shown in Figure 1, while a list of relevant bond lengths and angles is given in Table 1 together with those of **6′** (see next section) and **1** for comparison. The difference Fourier maps (see Experimental Section) unambiguously showed D atoms bonded to the ruthenium center while the site occupancy factors (s.o.f.) of the H atoms of the phosphines, left to refine unconstrained, did not differ significantly from 1.00, thus confirming that deuteration occurred only at the metal site. The refined deuteride s.o.f corresponds to an average deuteration of 90% in agreement with the NMR data. The coordination geometry of **5** does not differ from that of **1** with the two D_2 ligands making angles of 23.2(1)° and 24.7(1)° with respect to the coordination plane defined by the Ru1, D1h and D2h atoms (the corresponding values for **1** are 22.8(5)° and 24.6(5)°, respectively). We also note that there is no significant difference (at the 3σ level) between the H−H and D−D distances in **1** and **5** showing that there is no effect on the D−D separations upon H/D substitution.[3c,9]

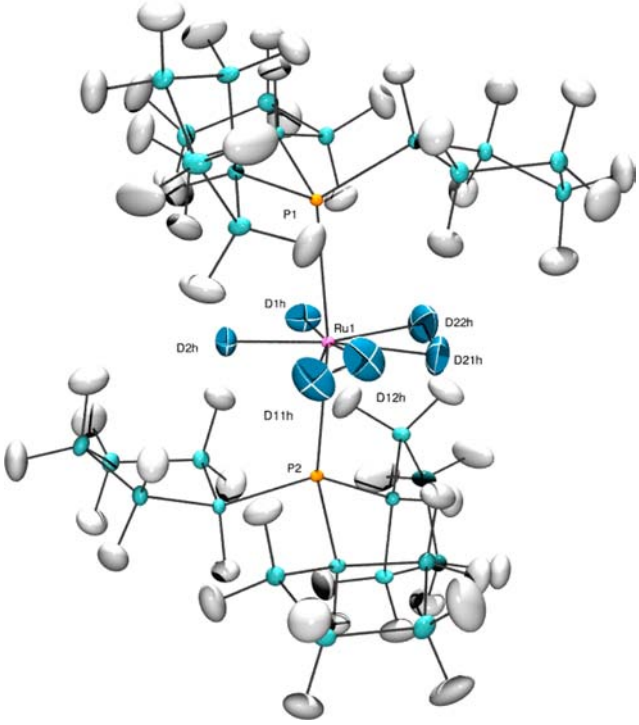

Figure 1. ORTEP view of the structure of $RuD_2(D_2)_2(P(C_5H_9)_3)_2$ (**5**) showing selective deuterium incorporation in the equatorial plane. Color code: H, gray; C, light blue; D, steel-blue. Ellipsoids drawn at 50% probability.

Table 1. Selected Bond Distances (Å) and Angles (deg) for Compounds 5, 6′, and 1[a]

	5	6′	1
Ru1−P1	2.3100(8)	2.310(3)	2.312(3)
Ru1−P2	3.3103(8)	2.305(3)	2.307(3)
Ru1−D1H	1.624(1)	1.622(3)	1.628(4)
Ru1−D2H	1.625(1)	1.618(3)	1.625(4)
Ru1−D11H	1.731(2)	1.730(4)	1.730(5)
Ru1−D12H	1.751(2)	1.750(4)	1.753(4)
Ru1−D21H	1.762(1)	1.766(4)	1.764(5)
Ru1−D22H	1.738(2)	1.737(4)	1.745(5)
D11H−D12H	0.840(2)	0.826(5)	0.825(8)
D21H−D22H	0.840(2)	0.824(5)	0.835(8)
P1−Ru1−P2	168.87(3)	168.9(1)	168.9(1)
P1−Ru1−D11*	91.41(4)	91.1(1)	91.4(2)
P1−Ru1−D22*	96.48(4)	96.5(1)	96.3(2)
P2−Ru1−D11*	95.93(4)	96.3(1)	96.0(2)
P2−Ru1−D22*	90.51(4)	90.5(1)	90.7(2)
D1H−Ru1−D2H	81.75(6)	81.9(2)	81.9(4)
D11*−Ru1−D22*	99.87(7)	99.1(2)	99.8(4)

[a]D11* and D22* are the midpoint of the D11−D12 and D21−D22 bonds, respectively.

Selective Deuteration at the Hydride and Dihydrogen Sites As Well As in the Cyclopentyl Rings of the Phosphines. Synthesis and Characterization of $[RuD_2(D_2)_2(P(Cyp\text{-}d_x)_3)_2]$. When monitoring over a few days a C_6D_6 solution of **5** by multinuclear NMR spectroscopy, we observed that, in addition to deuteration at the hydride and dihydrogen sites, monodeuteration occurred very selectively at the adjacent C3 and C3′ sites in the cyclopentyl rings. Incorporation of deuterium at the cyclopentyl sites is a much slower process, as illustrated by the spectra displayed in Figure 2. After 7 days, incorporation of about 12 deuterium atoms in the $PCyp_3$ rings was estimated by integrations from ^1H and ^2H NMR measurements (92.5% at the C3, C3′ sites), thus corresponding to $[RuD_2(D_2)_2(P(C_5H_7D_2)_3)_2]$ (**6**), a complex incorporating up to 18 deuterium atoms. Selective ^{13}C decoupling experiments demonstrate that incorporation of deuterium occurs very selectively at the C3, C3′ sites with the signal at δ 26.22 now resonating as a triplet with a $^1J_{CD}$ of 18.9 Hz from the $^{13}C\{^1H,^{31}P\}$NMR spectrum.[18] The two other ^{13}C signals for the CH (C1) and CH_2 (C2, C2′) groups do not show any deuterium coupling.

To obtain crystals suitable for neutron diffraction, another synthetic pathway had to be followed since the use of C_6D_6 solution prevented any crystallization attempts at low temperatures, as required for such highly soluble $PCyp_3$ species. Large crystals of the isotopolog **6′** were grown after workup from a pentane solution of **5** stirred for 3 days at room temperature and then pressurized under 3 bar D_2. As expected, the coordination geometry of complex **6′**, shown in Figure 3, is very similar to that of **5** (see Table 1). As for the latter complex, the D atoms bonded to the metal were found from a difference Fourier map and their s.o.f. refined without constraints resulting in an average occupancy of 0.91. In **6′**, the extent of deuterium incorporation is at an earlier stage than in **6** (see hereafter).

Moreover, the refinement of the occupancy factors of the H atoms in the cyclopentyl rings gave s.o.f. of 1.00 for all hydrogens except those bonded to the carbons in the C3 and C3′ positions of the cyp-rings (see Figure 3) for which the average occupancy was 0.26. These values show unambiguously and quantitatively the selective deuteration of the hydrides and of the H endo atoms facing the ruthenium at the C3, C3′ positions of the cyclopentyl rings and correspond to a degree of deuteration of 95% for the metal-bonded hydrogens and 32% for the C−H moieties.

The ^1H and ^2H NMR integration values from a C_6D_6 solution of **6′** (Supporting Information, Figure S4−S5) gave 95% D incorporation at the hydride sites and 36% at the C3, C3′ positions of the cyclopentyl rings, in agreement with the neutron data: thus in **6′**, the extent of deuterium incorporation

dx.doi.org/10.1021/ic302307m | Inorg. Chem. 2013, 52, 7329−7337

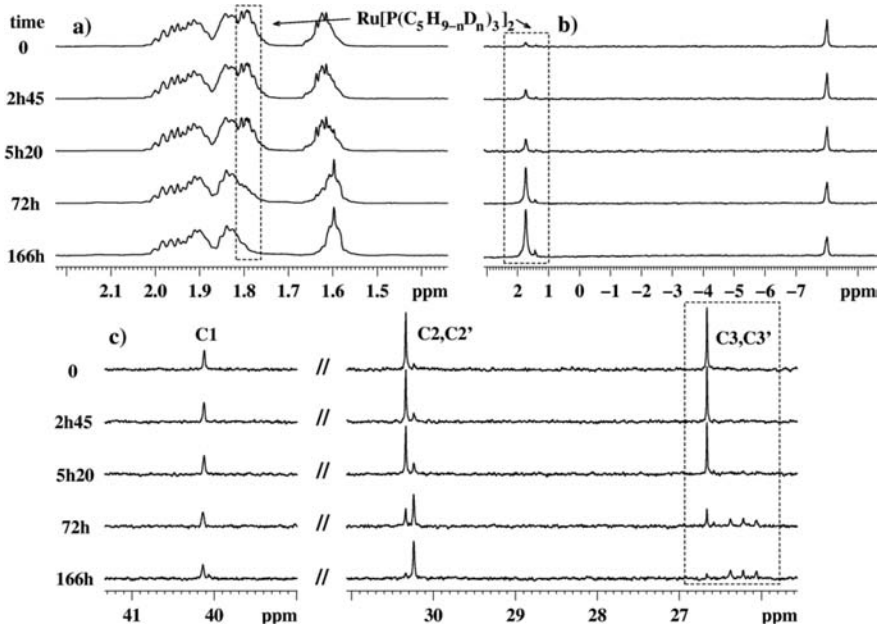

Figure 2. H/D exchange in a C_6D_6 solution of **5** at RT followed over one week by NMR spectroscopy. (a) ^1H NMR, cyclopentyl region; (b) ^2H NMR showing signal increase at δ 1.74; (c) $^{13}C\{^1H, ^{31}P\}$ NMR showing the 1:1:1 triplet resonance at δ 26.22.

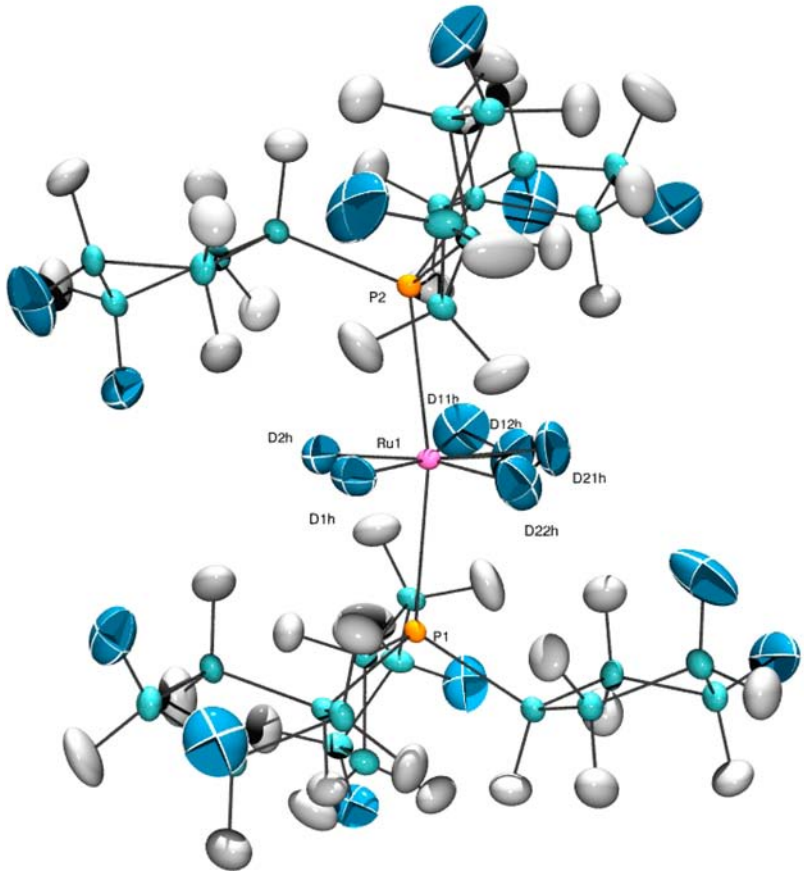

Figure 3. ORTEP view of the structure of **6′** showing selective deuterium incorporation in the equatorial plane as well as in the cyclopentyl C3, C3′ positions. Color code: H, gray; C, light blue; D, steel-blue.

is at an earlier stage than in **6** (36% vs 92.5% at the C3,C3′ sites).

Finally, the influence of the solvent was investigated. When monitoring a C_6D_6 solution of **1** over several days, the same reaction was observed as described above for the trans-formation of **5** into **6**. There is no need to isolate the intermediate **5**, and thus to use D_2 gas, to obtain deuterium incorporation into the cyclopentyl rings. In contrast, no change occurred in the NMR spectra of **1** kept for several days in a THF-d_8 solution (Supporting Information, Figure S23−25).

dx.doi.org/10.1021/ic302307m | *Inorg. Chem.* 2013, 52, 7329−7337

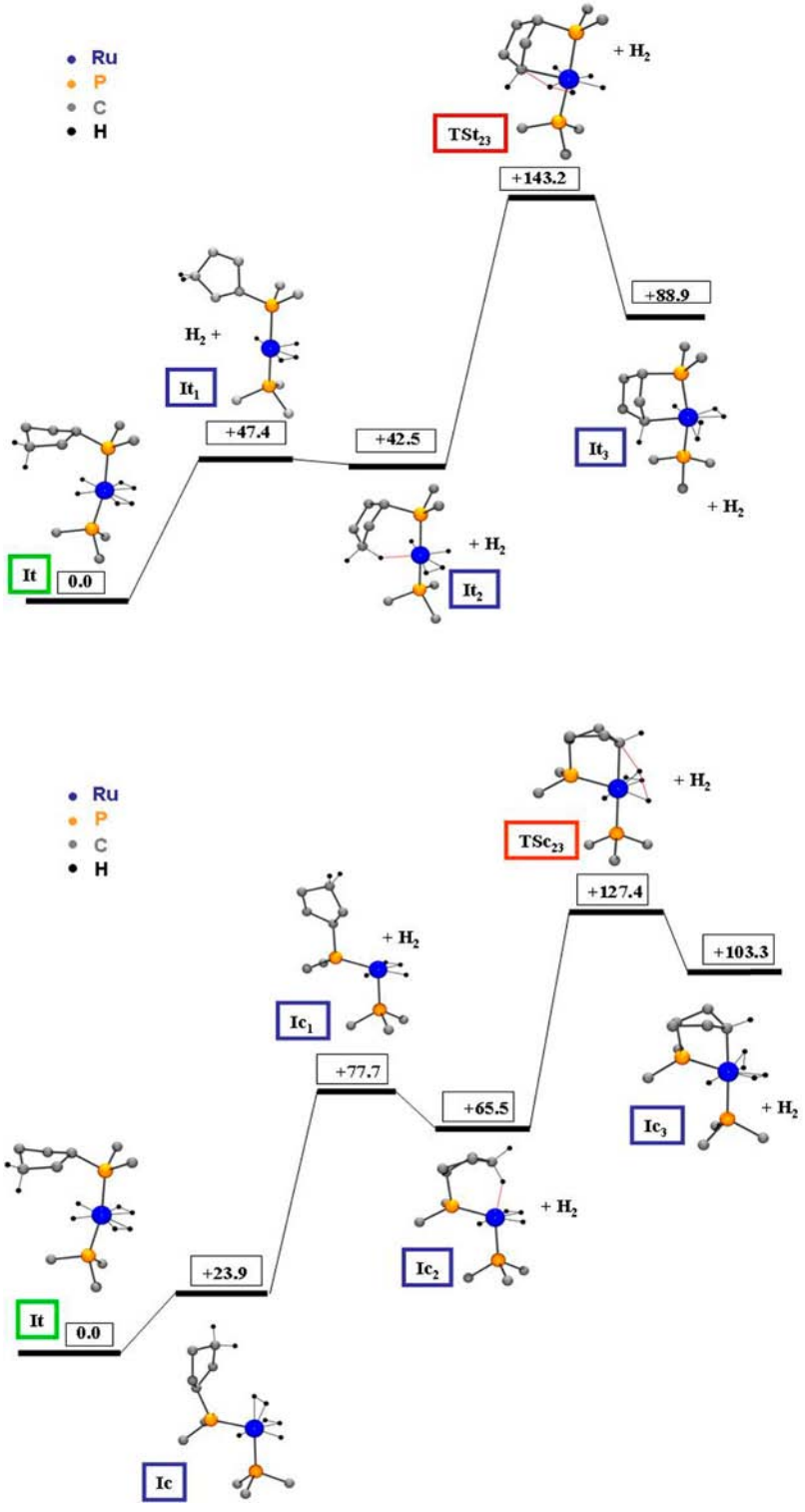

Figure 4. C−H activation pathways at the C3 site of one cyclopentyl ring from $[RuH_2(H_2)_2(P(C_5H_9)Me_2)(PMe_3)]$ (**It**). ***Top diagram***: phosphines in *trans* positions. ***Bottom diagram***: phosphine isomerization to *cis* positions. $\Delta_r G$ are given at 298 K in kJ mol^{-1}.

Apparently, although C−H activation can easily operate in the case of benzene, such a process is much more difficult for THF. In THF-d_8, for **1**, an exposure to 3 bar D_2 is required to achieve selective deuteration at the hydride and dihydrogen sites to form **5** (Supporting Information, Figure S26−28). Additional pressure of D_2 gas prevented further deuteration of the cyclopentyl rings, the compound remaining saturated with the electron count at the metal of 18 electrons, and with no vacant orbital for use in C−H bond activation (Supporting Information, Figure S29−31). However, when keeping a solution of **5** in THF-d_8 in the absence of a D_2 atmosphere, H/D exchange occurred in the cyclopentyl rings, resulting in hydrogen enrichment at the hydride/dihydrogen sites, whereas no change in the THF-d_8 residual signal was observed in the ^1H NMR spectra (Supporting Information, Figure S12). In this case, H/D exchange in the cyclopentyl rings only derived from

dx.doi.org/10.1021/ic302307m | *Inorg. Chem.* 2013, 52, 7329−7337

the deuterium atoms present in the equatorial plane of the starting complex **5**. Thus, there is evidence for an intramolecular H/D exchange process which is reversible through C−H activation.

It is worth considering the mechanistic features of C−H activation by the polyhydride rhenium complex, $ReH_7(PCy_3)_2$, as reported by Caulton and his group, as it is closely related to this work.[19] H/D exchange between $ReH_7(PCy_3)_2$ and C_6D_6 operated at 60−80 °C led after 1 h to the disappearance of the hydride signal in the ^1H NMR spectrum as well as to a decrease in the intensities of some cyclohexyl resonances together with an increase in the $C_6(H,D)_6$ resonance. Detailed analyses showed that mono deuteration occurred at the C2 and C3 positions of the cyclohexyl rings but with different rates. This ruled out a concerted ring dehydrogenation, and these authors favored a mechanism involving the transient $ReH_5(PCy_3)_2$ and metalation through oxidative addition at the C2 and C3 positions, the resulting five-membered ring being preferred to a four-membered ring in agreement with the difference in rates.

DFT Studies and Mechanism of the H/D Exchange Processes. DFT calculations were performed to obtain more detailed information on the C−H/C−D exchange process which occurred intramolecularly, whatever the solvent used. Several pathways were examined, but we will only detail the main route leading to C−H activation at the C3 positions (see Supporting Information for more details). The process was examined starting from $[RuH_2(H_2)_2(P(C_5H_9)Me_2)(PMe_3)]$ (**It**) as a model of complex **1**. Only one cyclopentyl ring was used to avoid any conformational problem. The main process is depicted in Figure 4. It may be found rather surprising that the lowest energy pathway is achieved through isomerization of the two bulky phosphines to the cis position (Figure 4 *bottom*). However, such a *cis* geometry was previously observed in the dihydride complex $[RuH_2\{(\eta^2\text{-}C_5H_7)PCyp_2\}_2]$ (**7**), an isolated intermediate for the formation of **3**.[11] Phosphine isomerization to **Ic** is followed by dihydrogen loss ($\mathbf{Ic_1}$). Subsequent C−H activation at the C3 position ($\mathbf{Ic_2}$) leads to ($\mathbf{Ic_3}$) with concomitant formation of a dihydrogen ligand, the ruthenium keeping the same oxidation state. The transition state $\mathbf{TSc_{23}}$ connects to $\mathbf{Ic_3}$ at 61.9 kJ mol^{-1} above $\mathbf{Ic_2}$. In contrast, keeping the phosphines in the *trans* position gives rise to $\mathbf{TSt_{23}}$ lying 100.7 kJ mol^{-1} above $\mathbf{It_2}$. The analysis of the motion associated with $\mathbf{TSc_{23}}$ indicates that this TS is mainly associated with the lengthening of the C−H bond and the dihydrogen bond formation. This is a typical illustration of the σ-CAM mechanism.[20] C−H bond breaking leads to a hydrido carbon−metalated species, $\mathbf{Ic_3}$, stabilized by two dihydrogen ligands. This pathway is reminiscent of the one described by Weller and MacGregor on the dehydrogenation of a monocyclopentylphosphine rhodium complex, with selective C−H activation at the C3, C3′ positions.[21] In our system, H/D exchange is then facile via dihydrogen rotation, a low-energy process. Indeed, we have measured the dihydrogen barrier to rotation in **1** by neutron incoherent inelastic scattering and found for the two H_2 ligands barriers of 4.14 and 4.56 kJ mol^{-1}, respectively.[22] The isomerization pathway through the phosphines in trans position (Figure 4 Top) involves an overall barrier of 15.8 kJ mol^{-1} (TSt_{23} vs TSc_{23}) above the cis route (Figure 4 Bottom) and thus might remain competitive for the real phosphine system.

CONCLUSION

We have demonstrated that selective incorporation of deuterium atoms in a ruthenium complex can be achieved under very mild conditions at room temperature. Our combined NMR and neutron diffraction studies prove the selectivity of the labeled sites. The extent of deuterium incorporation into the bis(dihydrogen) ruthenium complex **1** depends upon the nature of the solvent and the presence *or absence*, of D_2 gas. C_6D_6 solutions of **1** under an argon atmosphere lead to a high degree of deuterium incorporation in the organometallic species, whereas by exposing C_6D_6 solutions of **1** to 3 bar D_2, deuterium incorporation is limited to 6 atoms at the hydride and dihydrogen sites. The resulting d_6 isotopolog **5** was formally characterized both in solution by multinuclear NMR and in the solid state through neutron diffraction. Further deuterium incorporation can be achieved producing **6**, in which all the atoms in the equatorial plane are deuterium, and, additionally, each cyclopentyl ring has endo deuterium atoms cis located at the C3 and C3′ positions. Conformational aspects of the cyclopentyl rings are responsible for the selectivity of the labeling process occurring at the equivalent C3, C3′ cis positions as a result of a favored C−H approach to the metal center. Neutron diffraction on **6′** allows us to rule out a bimolecular process which would involve exo hydrogen atoms at the C3, C3′ positions. Moreover, rather counterintuitively, the use of D_2 gas is not always the best choice to increase deuterium incorporation in a given compound, as we show that in our system, D_2 gas can inhibit the C−H/C−D exchange process because the complex remains saturated with no vacant orbital accessible for C−H bond activation. One can see from this in-depth study, in solution by multinuclear NMR and in the solid state via neutron diffraction on **5** and **6′**, that labeling is highly dependent not only on the experimental conditions, but also on the nature of the putative "spectator" ligands. Here, the cyclopentyl rings of the phosphines provide an additional reservoir for deuterium incorporation through C−H activation.

EXPERIMENTAL SECTION

General Methods. All reactions and workup procedures were performed under an argon atmosphere using conventional vacuum line and Schlenk tube techniques or in a drybox. Solvents were dried according to standard procedures and degassed prior to use. C_6D_6 (supplier: Euriso-top; 99.5% D) was degassed and placed as received in a Schlenk tube containing activated 4 Å molecular sieves. THF-d_8 (supplier: Euriso-top; 99.5% D) was dried over sodium for one night followed by distillation (trap-to-trap techniques) and kept in a Schlenk tube containing activated 4 Å molecular sieves. $RuH_2(H_2)_2(PCyp_3)_2$ (**1**) was prepared according to a published procedure.[9] NMR spectra were acquired on a Bruker Avance 500 spectrometer. D_2 gas (purity: 99.9% with O_2 < 10 ppm; N_2 < 25 ppm, H_2O < 10 ppm) was purchased from Air Liquide and was used as received. D_2 pressurized NMR experiments were performed by using Quick Pressure Valve NMR tubes.[14]

NMR Experiments. The residual signal of benzene in C_6D_6 was calibrated at 7.27 ppm and used as a reference for ^1H NMR. The C_6D_6 signal in ^2H NMR was calibrated at 7.27 ppm. In the case of THF-d_8 experiments, the low-field signal was calibrated at 3.62 ppm. Deuterium incorporation was determined by using the 4 equations shown hereafter:

$$X_1 + X_2 = 54 \quad (1)$$

$$Y_1 + Y_2 = 6 \quad (2)$$

$$X_1/Y_1 = A \quad (3)$$

dx.doi.org/10.1021/ic302307m | Inorg. Chem. 2013, 52, 7329−7337

$$X_2/Y_2 = B \quad (4)$$

where X_1 is the number of H on the two $PCyp_3$ ligands; X_2 is the number of D on the two $PCyp_3$ ligands; Y_1 is the number of H coordinated to the metal center; Y_2 is the number of D coordinated to the metal center; A is the ratio between H on the two $PCyp_3$ ligands and the number of H coordinated to the metal center, determined from ^{1}H NMR integrations; B si the ratio between D on the two $PCyp_3$ ligands and the number of D coordinated to the metal center, determined from ^{2}H NMR integrations. The percentage of D incorporation in $PCyp_3$ is defined by $X_2/12$ (12 possible positions at C3 an C3′ sites available for H/D exchange).

Deuterium Incorporation in $RuH_2(H_2)_2(PCyp_3)_2$. *1. Synthesis and Characterization of $[RuD_2(D_2)_2(P(C_5H_9)_3)_2]$ (5).* In a glovebox under an Ar atmosphere, $RuH_2(H_2)_2(PCyp_3)_2$ (**1**) (500 mg, 0.857 mmol) was introduced into a 160 mL Fischer−Porter bottle, and 3 mL of pentane was added. The Fischer−Porter bottle was transferred outside the glovebox and was connected to the deuterium line. The solution was pressurized to 3 bar of D_2 and left to stir for 5 h at room temperature. After this time, the gas pressure was removed under vacuum and immediately the solution was pressurized again under 3 bar of D_2 and stirred for another 5h. This operation was repeated once prior to stirring overnight. The colorless solution was cooled below −30 °C, and a white precipitate appeared after a few minutes. After 30 min stirring, the pressure was released and D_2 replaced by an argon atmosphere. The suspension was kept cold during all these operations. The solution was then removed by a cannula equipped with a filter paper. After rapid drying under vacuum the solid $RuD_2(D_2)_2(PCyp_3)_2$ (**5**) (425 mg, 0.722 mmol, isolated yield 84%) was placed inside the glovebox and stored in the freezer at −37 °C. Crystals were obtained by dissolving the solid in a minimum of pentane; the solution was then introduced inside a screw-cap NMR tube and placed in the freezer at −37 °C. All these operations have to be done as quickly as possible. Crystals suitable for neutron diffraction techniques were obtained within a few hours. After crystallization, the solution was removed rapidly at low temperature. Selection of suitable crystals was done under an argon atmosphere inside a glovebox equipped with a binocular microscope. The selected crystals were introduced into special quartz capillary tubes supplied by ILL. The crystals were sent to ILL under cold conditions (below −10 °C).

^{1}H NMR (C_6D_6, 298 K, 500.33 MHz): −8.04 (m, residual ^{1}H, RuD_nH_{6-n}), 1.6−2.0 (H, $PCyp_3$)

^{2}H NMR (C_6D_6, 298 K, 76.8 MHz): − 8.0 (m, RuD_nH_{6-n}).

$^{13}C\{^1H,^{31}P\}$NMR (C_6D_6, 298 K, 125.8 MHz, 30 min after dissolution) 40.07 (s, PCH, $PCyp_3$), 30.34 (s, PCH-$\underline{C}H_2$, $PCyp_3$), 26.66 (s, PCH−CH_2-$\underline{C}H_2$, $PCyp_3$), $^{31}P\{^1H\}$ NMR (C_6D_6, 298 K, 202.54 MHz): 81.0 (s).

2. Synthesis and Characterization of $[RuD_2(D_2)_2(P(Cyp\text{-}d_x)_3)_2]$ (6′ and 6). **A.** In a glovebox under an Ar atmosphere, $RuD_2(D_2)_2(PCyp_3)_2$ (**5**) (220 mg, 0.373 mmol) was introduced into a 10 mL Fischer−Porter bottle, and 2.5 mL of pentane was added. The mixture was stirred for three days at room temperature. After this delay the bottle was transferred outside the glovebox and connected to the deuterium line. The solution was pressurized to 3 bar of D_2 and stirred for 3 h. The solution was then cooled down to −25 °C leading to the formation of a white precipitate. Gas pressure was released and pentane was removed under vacuum at this low temperature. The resulting white solid was transferred into the glovebox. Partial incorporation of deuterium inside the cyclopentyl rings was determined by NMR. Single crystals of **6′** suitable for neutron diffraction techniques were obtained and selected as described above for **5**.

B. To incorporate more deuterium at the C3, C3′ positions, a solution of **5** was kept for a few days in C_6D_6 solution at room temperature (7 days) to produce $RuD_2(D_2)_2(PCyp_3\text{-}d_6)_2$ (**6**).

$^{13}C\{^1H,^{31}P\}$ NMR (C_6D_6, 298 K, 125.8 MHz, 7 days after dissolution) 40.14 (s, PCH $PCyp_3$-d_6), 30.24 (s, PCH-$\underline{C}H_2$, $PCyp_3$-d_6), 26.22 (t, $^1J_{CD}$ = 18.9 Hz, PCH−CH_2-$\underline{C}HD$, PCyp),

^{2}H NMR (C_6D_6, 298 K, 76.8 MHz): 1.74 (bd s, PCyp-$d6$) − 8.01 (bd s, RuD_nH_{6-n}).

Neutron Data Collection and Refinement of (5) (CCDC 892258). A prismatic crystal, with a volume of about 12.1 mm^3, was mounted in an inert Ar atmosphere between two wads of quartz wool inside a thin-walled quartz tube, sealed with an O-ring to a purpose-designed Al base. The sample was mounted on a Displex cryorefrigerator,[23] on the ILL thermal-beam diffractometer D19 equipped with the new horizontally curved "banana-shaped" position-sensitive detector.[24] This detector is based on a multiwire gas counter technology (5 atm ^{3}He and 1 atm CF_4), with innovative use of an electrostatic lens to improve vertical resolution and electrodes deposited on glass plates consisting of 640 vertical anodes and 256 horizontal cathodes, with a nominal resolution of 1.56 mm vertically and 2.50 mm horizontally, and subtends 30 degrees vertically and 120 degrees horizontally. This detector is mounted symmetrically around the equatorial plane with a sample to detector distance of 76 cm. This new set up assures accurate and fast data collections even with "small size" crystals (≤1 mm^3). The chosen neutron wavelength was 1.1675 Å from the (311) planes of a Cu monochromator in reflection (at the high resolution 90° take-off angle). The crystal was cooled slowly (2 K/min) to 20 K while monitoring the diffraction pattern. No significant changes in the crystal mosaic or splitting of peaks were observed during cooling. The space group $P2_1/n$, as found for the starting complex $[RuH_2(H_2)_2(P(C_5H_9)_3)_2]$ (**1**), was confirmed at 20 K. The accessible intensities, up to $\theta \leq 61.27°$, were measured, to pre-set monitor counts, in a series of 80° ω scans, in steps of 0.07° and typical counting times of 10.5 s per step, to obtain reasonable counting statistics. A wide range of crystal orientations (different φ and χ positions) was used to cover reciprocal space with massive redundancy as a test of both the sample and the detector stability. Because of its large horizontal opening, only one detector position was required. Between the long scans, 6 strong reflections were monitored every 4 h in shorter scans, and showed no significant change.

The unit cell dimensions were calculated precisely (ILL program Rafd19) at the end of the data collection, from the centroids in 3D of 11259 strong reflections ($3.2 \leq \theta \leq 61.3°$). Raw intensity data were corrected for vertical and horizontal positional distortions and Bragg intensities were integrated in 3D using a new version of the program Retreat,[25] modified for the new detector geometry. The Bragg intensities were corrected for attenuation by the cylindrical aluminum and vanadium Displex heat-shields and analytically, using Gaussian grid, for the crystal absorption using the program D19abs (minimum and maximum transmission coefficients 0.4643 and 0.6425).[26] The starting structural model was based on the atomic coordinates from the neutron data refinement of (**1**), while the presence and positions of D atoms bonded to the Ru center were obtained from a difference Fourier map. Details of the crystallographic data are given in Table 2 and in the Supporting Information.

The structure was refined by full matrix least-squares, minimizing the function $[\sum w(F_o^2 - (1/k)F_c^2)^2]$ and using all the independent data. Anisotropic Displacement Parameters (ADPs) were used for all atoms while the site occupancy factors (s.o.f.) of H and D atoms were left to refine freely to determine the degree of deuteration in the sample.

The average s.o.f. of the D atoms bonded to the metal is 0.89 (corresponding to 90% deuteration) while for the phosphine H atoms it is not significantly different from 1.00 (set to 1.00 for the final refinement). For convenience, the deuterium occupancies were set to 1.00 in the calculations of the molecular formula and weight.

At the end of the refinement a difference Fourier map revealed the presence of a minor second conformation for the D_2 ligands, with the two dideuterium ligands almost perpendicular to each other (91.3°) and making angles of 106° and 41°, respectively, with the coordination plane defined by atoms Ru1, D1H, D2H (see Supporting Information, Figure S35). These additional atoms were included in the final refinement, using isotropic temperature factors and with the D−D distance constrained to 0.82(1) Å. The average occupancy factors for the "parallel" and "perpendicular" D_2 ligands are about 0.8 and 0.1 respectively. Upon convergence the final Fourier difference map showed no significant features.

dx.doi.org/10.1021/ic302307m | Inorg. Chem. 2013, 52, 7329−7337

Table 2. Crystal Data and Details of the Structure Refinement for (5) and (6′)

	5	6′
formula	$C_{30}H_{54}D_6P_2Ru$	$C_{30}H_{50}D_{10}P_2Ru$
mol weight	589.84	593.86
data coll T, K	20(1)	20(1)
crystal system	monoclinic	monoclinic
space group (no.)	$P2_1/n$ (14)	$P2_1/n$ (14)
a, Å	14.8292(1)	14.831(1)
b, Å	9.4260(1)	9.4259(6)
c, Å	21.6700(2)	21.675(2)
β, deg	105.384(1)	105.38(1)
volume, Å^3	2920.51(5)	2921.5(3)
Z	4	4
ρ_{calc}, g cm^{-3}	1.333	1.322
μ, mm^{-1}	0.320	0.298
no. data collected	27791	39595
no. independ data	9339	6699
no. obs. reflct. $\lvert F_o\rvert^2 > 2.0\sigma(\lvert F_o\rvert^2)$	8035	5415
no. param. refined	855	857
R_{int}	0.0331	0.0771
R $[I > 2\sigma(I)]^a$	0.0319	0.0635
R_w $[I > 2\sigma(I)]^a$	0.0606	0.1396
GOF^a	1.146	1.120

$^a R_{int} = \sum\lvert F_o^2 - \langle F_o^2\rangle\rvert/\sum F_o^2$; $R(F_o) = \sum\lvert\lvert F_o\rvert - \lvert F_c\rvert\rvert/\sum\lvert F_o\rvert$; $Rw(F_o^2) = [\sum w(F_o^2 - F_c^2)^2]/\sum w(F_o^2)^2]^{1/2}$; GOF = $[\sum[w(F_o^2 - F_c^2)^2]/(N - P)]^{1/2}$, where N, P are the number of observations and parameters, respectively.

Neutron Data Collection and Refinement of (6′) (CCDC 892259). The data collection, on a prismatic crystal with an approximate volume of 12.2 mm^3, was again carried out on the ILL D19 diffractometer as described above. The space group $P2_1/n$ was confirmed at 20 K. The chosen neutron wavelength was 1.3152 Å (Ge(115) monochromator). The intensities, up to $\theta \leq 59.5°$, were measured, with typical counting times of 7 s per step. Three standard reflections were monitored every 8 h and showed no significant change. The unit cell dimensions were calculated (Rafd19) at the end of the data collection, from the centroids in 3D of strong reflections ($2.8 \leq 2\theta \leq 118.5°$). Raw intensity data were processed as above. The Bragg intensities were corrected for attenuation by the cylindrical aluminum and vanadium Displex heat-shields (minimum and maximum transmission coefficients 0.8979 and 0.9651). The starting structural model was the same as used for (5). The structure was refined by full matrix least-squares, as described above, using ADPs for all atoms. The s.o.f. of all H/D atoms were refined without constraints. The average s.o.f. for the D atoms bonded to the metal center is 0.91. For the phosphine-hydrogens the s.o.f. were equal to 1.00 with the exception of the H atoms bonded to the C3 and C3′ atoms of the cyclopentyl rings whose average s.o.f. is 0.26. Analogous results were obtained by refining the H/D occupancies under the constraint that total occupancy (H + D) for each C3 and C3′ site should be equal to 1.0.

These refined values correspond to a deuteration of 95% for the deuterides and 32% for the C−H moieties. Upon convergence the final Fourier difference map showed no significant features. Taking into account the values for the deuteration both at the metal and in the rings a molecular formula $C_{30}H_{50}D_{10}P_2Ru$ was assumed and used for the molecular weight, density, and absorption coefficient calculations.

For both structures, the coherent scattering amplitudes used were those tabulated by Rauch and Waschkowski,[27] while the calculations were carried out using programs SHELX-97,[28] WINGX,[29] ORTEP,[29] and MERCURY.[303030] Further crystallographic data and geometrical parameters are given in the Supporting Information and as cif files.

Computational Details. They are given in the Supporting Information.

■ ASSOCIATED CONTENT

Supporting Information

NMR data: multinuclear NMR spectra for **5** (Figure S1−S3), **6′** (Figure S4,S5), and **6** (Figure S6−S8), solvent effects (C_6D_6 and THF-d_8) as a function of time (Figure S9−S31). Computational details (methods and Figure S32−S34). Neutron figure (S35) and tables (Tables S1−S7). This material is available free of charge via the Internet at http://pubs.acs.org.

■ AUTHOR INFORMATION

Corresponding Author

*E-mail: grellier@lcc-toulouse.fr (M.G.), alberto.albinati@unimi.it (A.A.), sylviane.sabo@lcc-toulouse.fr (S.S.-E.).

Author Contributions

The manuscript was written through contributions of all authors. All authors have given approval to the final version of the manuscript.

Notes

The authors declare no competing financial interest.

■ ACKNOWLEDGMENTS

We thank the CNRS and the ANR (programme blanc HyBoCat ANR-09-BLAN-0184) for support (M.G., Y.C., S.S.E.). Johnson Matthey is gratefully acknowledged for a generous loan of $RuCl_3{\cdot}nH_2O$. Computer time was given by the HPC resources of CALMIP (Toulouse, France) under the allocation 2012-[P0909]. A.A. and S.R. acknowledge support from the MIUR-PRIN 2009 project.

■ REFERENCES

(1) (a) Atzrodt, J.; Derdau, V.; Fey, T.; Zimmermann, J. *Angew. Chem., Int. Ed.* **2007**, *46*, 7744−7765. (b) Heazlewood, B. R.; Maccarone, A. T.; Andrews, D. U.; Osborn, D. L.; Harding, L. B.; Klippenstein, S. J.; Jordan, M. J. T.; Kable, S. H. *Nat. Chem.* **2011**, *3*, 443−448. (c) Campos, J.; Rubio, M.; Esqueda, A. C.; Carmona, E. *J. Labelled Compd. Radiopharm.* **2012**, *55*, 29−38. (d) Neubert, L.; Michalik, D.; Bähn, S.; Imm, S.; Neumann, H.; Atzrodt, J.; Derdau, V.; Holla, W.; Beller, M. *J. Am. Chem. Soc.* **2012**, *134*, 12239−12244.

(2) (a) Shao, L.; Hewitt, M. C. *Drug News Perspect.* **2010**, *23*, 398−404. (b) Hanson, J. R. *Organic Chemistry of Isotopic Labelling*; RSC Publishing: Cambridge, U.K., 2011. (c) Baldwin, J. E.; Kostikov, A. P. *J. Org. Chem.* **2010**, *75*, 2767−2775. (d) Gath, J.; Hoaston, G. L.; Vold, R. L.; Berthoud, R.; Coperet, C.; Grellier, M.; Sabo-Etienne, S.; Lesage, A.; Emsley, L. *Phys. Chem. Chem. Phys.* **2009**, *11*, 6962−6971. (e) Hoang, T. K. A.; Hamaed, A.; Moula, G.; Aroca, R.; Trudeau, M.; Antonelli, D. M. *J. Am. Chem. Soc.* **2011**, *133*, 4955−4964. (f) Prins, R. *Chem. Rev.* **2012**, *112*, 2714−2738.

(3) (a) Gómez-Gallego, M.; Sierra, M. A. *Chem. Rev.* **2011**, *111*, 4857−4963. (b) Blum, S. A.; Tan, K. L.; Bergman, R. G. *J. Org. Chem.* **2003**, *68*, 4127−4137. (c) Heinekey, D. M. *J. Labelled Compd. Radiopharm.* **2007**, *50*, 1063−1071. (d) Kubas, G. J. *Metal Dihydrogen and [sigma]-bond Complexes*; Kluwer Academic: Dordrecht, The Netherlands, 2001. (e) Pike, S. D.; Thompson, A. L.; Algarra, A. G.; Apperley, D. C.; Macgregor, S. A.; Weller, A. S. *Science* **2012**, *337*, 1648−1651.

(4) (a) Parkin, G. *J. Labelled Compd. Radiopharm.* **2007**, *50*, 1088−1114. (b) Lockley, W. J. S.; Heys, J. R. *J. Labelled Compd. Radiopharm.* **2010**, *53*, 635−644 , and all the papers in this special issue. (c) Gunnoe, T. B. In *Physical Inorganic Chemistry: Principles, Methods, and Models*; Bakac, A., Ed.; John Wiley & Sons: Hoboken, NJ, 2010; pp 495−549. (d) Jones, W. D.; Feher, F. J. *J. Am. Chem. Soc.* **1985**, *107*, 620−631. (e) Zou, F.; Furno, F.; Fox, T.; Schmalle, H. W.; Berke, H.; Eckert, J.; Chowdhury, Z.; Burger, P. *J. Am. Chem. Soc.* **2007**, *129*, 7195−7205.

(5) (a) Albinati, A.; Cesarotti, E.; Mason, S. A.; Rimoldi, I.; Rizzato, S.; Zerla, D. *Tetrahedron: Asymmetry* **2010**, *21*, 1162−1165. (b) Rizzato, S.; Bergès, J.; Mason, S. A.; Albinati, A.; Kozelka, J. *Angew. Chem., Int. Ed.* **2010**, *49*, 7440−7443. (c) Shima, T.; Luo, Y.; Stewart, T.; Bau, R.; McIntyre, G. J.; Mason, S. A.; Hou, Z. *Nat. Chem.* **2011**, *3*, 814−820.
(6) (a) Crabtree, R. H.; Felkin, H.; Morris, G. E. *J. Organomet. Chem.* **1977**, *141*, 205−215. (b) Nilsson, G. N.; Kerr, W. J. *J. Labelled Compd. Radiopharm.* **2010**, *53*, 662−667. (c) Yung, C. M.; Skaddan, M. B.; Bergman, R. G. *J. Am. Chem. Soc.* **2004**, *126*, 13033−13043. (d) Iluc, V. M.; Fedorov, A.; Grubbs, R. H. *Organometallics* **2011**, *31*, 39−41. (e) Hebden, T. J.; Goldberg, K. I.; Heinekey, D. M.; Zhang, X.; Emge, T. J.; Goldman, A. S.; Krogh-Jespersen, K. *Inorg. Chem.* **2010**, *49*, 1733−1742.
(7) (a) Lau, C. P.; Ng, S. M.; Jia, G.; Lin, Z. *Coord. Chem. Rev.* **2007**, *251*, 2223−2237. (b) Chaudret, B. *J. Organomet. Chem.* **1984**, *268*, c33−c37. (c) Tse, S. K. S.; Xue, P.; Lin, Z.; Jia, G. *Adv. Synth. Catal.* **2010**, *352*, 1512−1522. (d) Gusev, D. G.; Hübener, R.; Burger, P.; Orama, O.; Berke, H. *J. Am. Chem. Soc.* **1997**, *119*, 3716−3731. (e) Ayed, T.; Barthelat, J.-C.; Tangour, B.; Pradère, C.; Donnadieu, B.; Grellier, M.; Sabo-Etienne, S. *Organometallics* **2005**, *24*, 3824−3826. (f) Callaghan, P. L.; Fernandez-Pacheco, R.; Jasim, N.; Lachaize, S.; Marder, T. B.; Perutz, R. N.; Rivalta, E.; Sabo-Etienne, S. *Chem. Commun.* **2004**, 242−243. (g) Kubas, G. J. In *Hydrogen-Transfer Reactions*; Hynes, J. T., Klinman, J. P., Limbach, H. H., Schowen, R. L., Eds.; Wiley-VCH: Weinheim, Germany, 2006. (h) Kovacs, G.; Nadasdi, L.; Laurenczy, G.; Joo, F. *Green Chem.* **2003**, *5*, 213−217.
(8) (a) Douglas, T. M.; Weller, A. S. *New J. Chem.* **2008**, *32*, 966−969. (b) Grellier, M.; Sabo-Etienne, S. *Chem. Commun.* **2012**, *48*, 34−42.
(9) Grellier, M.; Vendier, L.; Chaudret, B.; Albinati, A.; Rizzato, S.; Mason, S.; Sabo-Etienne, S. *J. Am. Chem. Soc.* **2005**, *127*, 17592−17593.
(10) Alcaraz, G.; Grellier, M.; Sabo-Etienne, S. *Acc. Chem. Res.* **2009**, *42*, 1640−1649.
(11) Grellier, M.; Vendier, L.; Sabo-Etienne, S. *Angew. Chem., Int. Ed.* **2007**, *46*, 2613−2615.
(12) Borowski, A. F.; Sabo-Etienne, S.; Christ, M. L.; Donnadieu, B.; Chaudret, B. *Organometallics* **1996**, *15*, 1427−1434.
(13) For initial papers dealing with C-H activation in cyclopentyl phosphines, see: (a) Miller, T. M.; Whitesides, G. M. *Organometallics* **1986**, *5*, 1473−1480. (b) Brainard, R. L.; Miller, T. M.; Whitesides, G. M. *Organometallics* **1986**, *5*, 1481−1490.
(14) Reguillo, R.; Grellier, M.; Vautravers, N.; Vendier, L.; Sabo-Etienne, S. *J. Am. Chem. Soc.* **2010**, *132*, 7854−7855.
(15) Guari, Y.; Castellanos, A.; Sabo-Etienne, S.; Chaudret, B. *J. Mol. Catal. A: Chem.* **2004**, *212*, 77−82.
(16) (a) Borowski, A. F.; Donnadieu, B.; Daran, J.-C.; Sabo-Etienne, S.; Chaudret, B. *Chem. Commun.* **2000**, 543−544. (b) Sabo-Etienne, S.; Chaudret, B. *Coord. Chem. Rev.* **1998**, *178*, 381−407.
(17) Walaszek, B.; Adamczyk, A.; Pery, T.; Yeping, X.; Gutmann, T.; Amadeu, N. d. S.; Ulrich, S.; Breitzke, H.; Vieth, H. M.; Sabo-Etienne, S.; Chaudret, B.; Limbach, H.-H.; Buntkowsky, G. *J. Am. Chem. Soc.* **2008**, *130*, 17502−17508.
(18) Wesener, J. R.; Moskau, D.; Guenther, H. *J. Am. Chem. Soc.* **1985**, *107*, 7307−7311.
(19) Zeiher, E. H. K.; DeWit, D. G.; Caulton, K. G. *J. Am. Chem. Soc.* **1984**, *106*, 7006−7011.
(20) Perutz, R. N.; Sabo-Etienne, S. *Angew. Chem., Int. Ed.* **2007**, *46*, 2578−2592.
(21) Douglas, T. M.; Brayshaw, S. K.; Dallanegra, R.; Kociok-Köhn, G.; Macgregor, S. A.; Moxham, G. L.; Weller, A. S.; Wondimagegn, T.; Vadivelu, P. *Chem.—Eur. J.* **2008**, *14*, 1004−1022.
(22) Albinati, A.; Georgiev, P. A.; Ollivier, J.; Grellier, M.; Sabo-Etienne, S., manuscript in preparation.
(23) Archer, J. M.; Lehmann, M. S. *J. Appl. Crystallogr.* **1986**, *19*, 456−458.
(24) Buffet, J. C.; Clergeau, J. F.; Cooper, R. G.; Darpentigny, J.; De Laulany, A.; Fermon, C.; Fetal, S.; Fraga, F.; Guerard, B.; Kampmann, R.; Kastenmueller, A.; Mc Intyre, G. J.; Manzin, G.; Meilleur, F.; Millier, F.; Rhodes, N.; Rosta, L.; Schooneveld, E.; Smith, G. C.; Takahashi, H.; Van Esch, P.; Van Vuure, T. L.; Zeitelhack, K. *Nuclear Instrum. Methods Phys. Res. A* **2005**, *554*, 392−405.
(25) Wilkinson, C.; Khamis, H. W.; Stansfield, R. F. D.; McIntyre, G. J. *J. Appl. Crystallogr.* **1988**, *21*, 471−478.
(26) Matthewman, J. C.; Thompson, P.; Brown, P. J. *J. Appl. Crystallogr.* **1982**, *15*, 167−173.
(27) Rauch, H.; Waschkowski, W. *Neutron Scattering Lengths. in Neutron Data Booklet*; 2nd ed.; Dianoux, A.-J., Lander, G., Eds.; Institut Laue-Langevin: Grenoble, France, 2003; http://www.ill.eu
(28) Sheldrick, G. M. *Acta Crystallogr.* **2008**, *A64*, 112−122.
(29) (a) Farrugia, L. J. *J. Appl. Crystallogr.* **1999**, *32*, 837−838. (b) Farrugia, L. J. *J. Appl. Crystallogr.* **1997**, *30*, 565.
(30) *Mercury CSD 3.0.1* (Build RC6); The Cambridge Crystallographic Data Center: Cambridge, U.K., 2011.